14th International Conference on Applications of Statistics and Probability in Civil Engineering, ICASP14
Dublin, Ireland, July 9-13, 2023

Probabilistic Flood Hazard Maps: A Bayesian Approach

Mariano Balbi
PhD candidate, Laboratorio de Materiales y Estructuras, Universidad de Buenos Aires, Buenos Aires, Argentina

David C. B. Lallemant
Assistant Professor, Asian School of the Environment, Nanyang Technological University, Singapore

ABSTRACT: The inclusion of epistemic uncertainties in flood hazard assessments can significantly impact estimates and the corresponding decision-making process. We propose a simulation approach to robustly account for these sources of uncertainty, while developing useful probabilistic output of flood hazard for further risk assessments. An extreme-value bayesian analysis is performed for future events simulation, and a pseudo-likelihood probabilistic approach for the calibration of the inundation model is used to compute uncertain water depths. The predictive posterior annual probability of exceedance is used to develop hazard maps that account for epistemic uncertainties. Results are compared to traditional hazard maps, showing that differences grow with increasing return period.

1. INTRODUCTION

Flood hazard is typically defined as the probability of exceedance of an intensity measure (IM) level at any point of interest during a given period of time. This usually comes in the form of 'hazard curves' that relate IM levels with an annual exceedance probability (AEP) or a mean time of recurrence, also known as return period (RP). In practice, the outcome is best conveyed through flood hazard maps for different RPs since we are typically interest in a continuous spatial region for risk analysis.

From a modelling perspective, hazard curves are the result of the convolution of two distinct models: a 'recurrence model' that describes the probability of occurrence of extreme events, such as an extreme rainfall, river discharge, or sea-level rise; and a 'source-to-site propagation model' (or just propagation model for brevity) that represents how the triggering event is translated into a spatial (and temporal) distribution of IM levels. The former is inherently probabilistic and typically modelled via standard stochastic time process such as the Poisson process. The propagation model, on the other hand, is typically modelled through deterministic physics-based models such as a hydrologic and/or a hydraulic inundation model.

The classical method involves computing the event's magnitude, such as peak discharge in riverine flooding, for different RPs and use it as input of the inundation model to develop flood maps for different recurrences. This is done using appropriately calibrated recurrence curves and inundation simulators based on available data and expert's knowledge. Simple as it is, it has widespread use along industry and academy. It does, however, implies the simplification that the models used are perfectly 'true'. The only probabilistic nature of the approach comes from the inherent uncertainty in the future occurrence of extreme events; also termed 'aleatory uncertainty' (Hall and Solomatine (2008)).

A broad range of researchers during the last decades have brought attention to the importance of including other sources of uncertainty into risk analysis in general, and flood hazard modelling in particular (Hall and Solomatine (2008)). Model-dependent uncertainties, also termed here 'epistemic', can arise from the data we use to constrain our models, our lack of knowledge regarding the true physical processes involved, or our limited analytic and computational capabilities for providing results (Hall and Solomatine (2008)). As a result of this, there is no simple translation from the 100yr discharge event to the 100yr flood depths map as the traditional approach would suggest.

The challenge of including epistemic uncertainties in flood hazard models, specifically in riverine floods, has drawn the attention of many researchers in the last decades. Some works have focused mainly on dealing with uncertain representations of the input discharge events for different return periods. This includes accounting for statistical fitting errors due to limited-length data and distribution family (Apel et al. (2008); Aronica et al. (2012); Romanowicz and Kiczko (2016); Stephens and Bledsoe (2020)), secondary input variables such as flood volume (Candela and Aronica (2017)), or more general hydrograph shape uncertainties through hydrological modelling Ahmadisharaf et al. (2018); Zahmatkesh et al. (2021). Others have focused on including uncertainty in the inundation model through its most sensitive parameters such as roughness coefficients (Aronica et al. (2012); Kiczko et al. (2013); Romanowicz and Kiczko (2016)), Digital Elevation Maps (DEM) (Apel et al. (2008)), or cross-section geometrical properties (Stephens and Bledsoe (2020)). Many of these have included both the epistemic uncertainties in the discharges recurrence as well as in the inundation model (Apel et al. (2008); Aronica et al. (2012); Kiczko et al. (2013); Romanowicz and Kiczko (2016); Stephens and Bledsoe (2020); Zahmatkesh et al. (2021)).

The typical outcome from most of these approaches is in the form of 'probability of flood' maps for different RPs. That is, for a nominal return period, different discharges and/or inundation model parameters are randomly sampled and used to obtain an ensemble of flood maps from which probability of flooding is computed empirically (Kiczko et al. (2013); Stephens and Bledsoe (2020); Zahmatkesh et al. (2021)). From the perspective of a damage assessment, this input is not very meaningful, and it is not directly applicable in standard vulnerability models. For this reason, instead of translating uncertain flow discharges for a given RP into a probability map (broadly known as 'event-based' approach), some researchers have aimed to develop recurrence curves for flood depths at the points of interest (Aronica et al. (2012); Nuswantoro et al. (2016); Romanowicz and Kiczko (2016)). This is generally done by simulating many possible events and computing the associated flood depth for each (Aronica et al. (2012); Nuswantoro et al. (2016)). A frequency analysis is later used to compute the RP for any flood depth level at any point of interest, thus, avoiding the assumption that the uncertain T-years event originates an uncertain T-years flood map.

The literature review indicates a lack of hazard methodologies that can (1) include epistemic uncertainties in both the recurrence and inundation models, (2) provide useful output for further risk assessments, while (3) also being probabilistically consistent and robust. This work explores a simulation methodology of flood scenarios using a Bayesian approach of extreme value theory and the GLUE framework to account for epistemic uncertainties in the recurrence model and the inundation simulator respectively. We propose the use of the posterior predictive probability of exceedance as a point measure of flood hazard that includes epistemic uncertainties in models (Fawcett and Green (2018)). A small case study of riverine flooding is used as a working example to test this methodology and obtained hazard curves and maps are compared to the traditional approach (i.e. no epistemic uncertainties).

2. METHODOLOGY

Under some simplifying assumptions, flood hazard can be computed by standard theory of Homogeneous Poisson Process. This model states that events occur with exponentially distributed inter-arrival times with a mean rate λ_0 that is constant over time. The mean annual rate of exceedance of

IM level z is given by Eq. (1).

$$\lambda(z) \approx \lambda_0 p(Z \geq z) \tag{1}$$

Since direct observations of water depths during flood events are very rare, probabilistic modelling of Z is usually done via mechanistic fluid dynamics models, here called simply inundation model or simulator. This model depends on a number of boundary conditions ν, such as the upstream river discharge and channel geometry, and a set of calibration parameters β, such as the soil roughness parameters.

$$Z = S(\nu, \beta) \tag{2}$$

The exceedance distribution of Z con then be computed conditioned on the probability distribution of ν, as per Eq. (3). This represents a more useful expression than Eq. (1) as long as a reliable source of observations for ν is available. This is the typical case in flood hazard, where we usually have historical measurements of river flow discharges or rainfall intensity.

$$p(Z \geq z) = \int_{\nu} \mathbf{1}\{S(\nu, \beta) \geq z\}\, p(\nu|\theta)\, d\nu \tag{3}$$

Where θ is the set of parameters that describe the probability distribution.

By introducing Eq. (3) into Eq. (1), we obtain the full expression for the flood hazard. This estimate can be thought of as conditioned on the parameters used to describe the inundation simulator β, and those to describe the recurrence of the events as λ_0 and θ. This is explicitly described in Eq. (4).

$$\lambda(z|\beta, \lambda_0, \theta) \approx \int \underbrace{\mathbf{1}\{S(\nu, \beta) \geq z\}}_{\substack{\text{Propagation}\\ \text{model}}} \underbrace{\lambda_0 p(\nu|\theta)}_{\substack{\text{Recurrence}\\ \text{model}}} d\nu \tag{4}$$

Epistemic uncertainties can arise due to limited data, limited knowledge, or simplifying assumptions over the process representation. In general, assuming that there is no structural modelling errors, we can assume that epistemic uncertainty can be represented by a probability distribution of the uncertain parameters for appropriately chosen models $p(.)$ and $S(.)$ (Beven (2014)).

An estimate of the hazard that includes these sources of uncertainty can obtained by integrating out the probability distributions of the models' parameters as described in Eq. (5). This is also known as predictive posterior estimate in the theory of Bayesian statistics (Gelman et al. (2013)).

$$\lambda(z|x) = \int_{\Theta} \lambda(z|\beta, \lambda_0, \theta)\, p(\Theta|x)\, d\Theta \tag{5}$$

Where x is the observed data, $\Theta = \{\beta, \lambda_0, \theta\}$, and $p(\Theta|x)$ is the posterior distribution.

In the following sub-sections we describe the methodology to estimate the probability distributions for these parameters, and the propagation algorithm to compute the hazard estimates.

2.1. *A Bayesian recurrence model*

The model for event's occurrence λ_0 and magnitude distribution $p(\nu)$ can be obtained from statistical analysis of time series of past events. Poisson Point Process theory as a generalization of the well-known Peaks-Over-Threshold (POT) methodology provides a robust methodology for this (Bezak et al. (2014)). Extreme events are individualized from historical records of daily discharges, by selecting an appropriate minimum threshold and time separation to ensure independence (Bezak et al. (2014)). A Generalized Pareto Distribution (GPD) is used as the model for discharge levels ν.

The predictive posterior distribution of the discharge for any given event, is then computed as per Eq. (6).

$$p(\nu|\hat{\nu}) = \int p(\nu|\xi, \sigma)\, p(\xi, \sigma|\hat{\nu})\, d\xi d\sigma \tag{6}$$

Where ξ and σ are the shape and scale parameters of the GPD respectively, and $\hat{\nu}$ are the observations of past extreme peak discharges.

The distribution $p(\xi, \sigma|\hat{\nu})$ is called the posterior distribution of the parameters and is obtained as

$$p(\xi, \sigma|\hat{\nu}) \propto p(\hat{\nu}|\xi, \sigma) \cdot p(\xi, \sigma) \tag{7}$$

Where $p(\hat{\nu}|\xi, \sigma)$ is the likelihood of the data, and $p(\xi, \sigma)$ is the prior distribution for the parameters.

A non-informative prior is used for the shape and scale parameters of the GPD as defined in Castellanos and Cabras (2007) as per Eq. (8).

$$p(\xi, \sigma) \propto \sigma^{-1}(1+\xi)^{-1}(1+2\xi)^{-1/2} \tag{8}$$

Valid for $\xi > -0.5$ and $\sigma > 0$.

The posterior distribution of the GPD's parameters is then given by Eq. (9).

$$f(\xi,\sigma|\hat{v}) \propto f(\xi,\sigma)\prod_{i=1}^{n}(1+\hat{v}_i\xi/\sigma)^{-(1+\xi)/\xi} \quad (9)$$

Finally, since arrivals between events are assumed to have an Exponential distribution with mean λ_0, we can assume a weakly informative $Gamma(1/2,1/2)$ prior which is the conjugate for the Poisson rate likelihood (Gelman et al. (2013)). In this case, the predictive posterior of the mean rate has a closed form solution as a *Gamma* distribution.

$$p(\lambda_0|\hat{v}) = Gamma(n+1/2, T+1/2) \quad (10)$$

Where n is the number of events and T is the number of years in the series.

2.2. *Probabilistic inundation model*

Epistemic uncertainties in the inundation simulator might come from lack of sufficient information to calibrate the parameters, observation errors, mechanistic simplifying assumptions, and numerical simplification of the equations solver (Kennedy and O'Hagan (2001)). We assume here, due to simplicity, that for a given simulator $S(.)$ these can be represented by uncertainty in the model's parameters β.

In the present work, epistemic uncertainty in the inundation model will be represented by probability distributions in the roughness parameters of the model. These distributions will be obtained by means of the GLUE framework, where all possible sets of parameters are assigned a normalized score (i.e. pseudo-likelihood) from an appropriately selected scoring rule. In the case of flood extent binary observations, it is typical to use the F-score, a variant of the classical Jaccard Index (Aronica et al. (2012)).

$$F(\beta) = \frac{A-B}{A+B+C} \quad (11)$$

Where A is the number of correctly predicted pixels, B the number of over-predicted pixels (predicted flooded observed non-flooded), and C is the number of under-predicted pixels (predicted non-flooded, observed flooded).

To build a likelihood distribution from the score in Eq. (11), three steps are typically followed: (1) compute a rescaled F_0 score so that it lies in the $[0,1]$ range to ensure positivity; (2) reject all 'non-behavioral' models by assigning $F_0 = 0$ according to a predefined acceptance threshold; and (3) standardize the resulting F-scores so that they all integrate to 1.

2.3. *Flood hazard*

Computing the integral from Eq. (5) requires numerical procedures since no analytic solution exists. A standard Monte-Carlo (MC) simulation approach relies on simulating N values of Z at the point of interest, and empirically computing the exceedance probability. Thus, an empirical estimate of flood hazard for a given set of model's parameters Θ_i can be numerically calculated as Eq. (12).

$$\lambda_i(z|\Theta_i) = \lambda_{0i}\frac{1}{N}\sum_j \mathbf{1}\left\{S\left(v_j,\beta_i\right) \geq z\right\} \quad (12)$$

The predictive posterior estimate can be obtained by averaging Eq. (12) over a simulation of M samples of the models parameters Θ.

$$\overline{\lambda}_i(z) = \frac{1}{M\cdot N}\sum_i \lambda_{0i}\sum_j \mathbf{1}\left\{S\left(v_j,\beta_i\right) \geq z\right\} \quad (13)$$

While complete and robust, this implies a very large number of evaluations of the inundation simulator that is computationally demanding. If we are only interested in the predictive posterior value of the flood hazard, rather than the individual contribution of each parameter to the uncertainty, we can rely on a single, sufficiently long simulation of events. Each event is simulated from a random sample of Θ as described here:

- While $t \leq T$:
    1. Sample λ_{0i}, ξ_i, σ_i, and θ_i from their posterior distributions.
    2. Sample the time to the next event's arrival T_i from $\exp(\lambda_{0i})$. Compute the cumulative time $t = \sum_{\forall i} T_i$
    3. Generate a discharge value v_i for the current event from GPD (ξ_i, σ_i)
    4. Compute water depth Z_i at all points of interest from $S(v_i, \theta_i)$

Where T is the desired time-length of the simulation.

3. CASE STUDY

The case study is based on a short reach on the upper river Thames in Oxfordshire, England, just downstream from a gauged weir at Buscot (Figure 1). The river at this reach has an estimated bankfull discharge of 40 m^3/s and drains a catchment of approximately 1000 km^2. The topography DEM was obtained from stereophotogrammetry at a 50 m scale with a vertical accuracy of ± 25 cm, obtained from large-scale UK Environment Agency maps and surveys. This reach has also been study previously by Aronica et al. (2002).

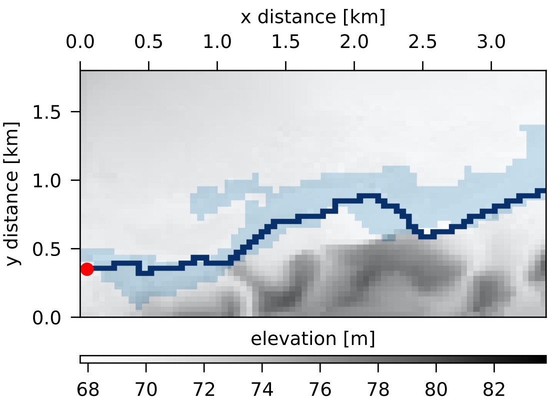

Figure 1: Floodplain topography at Buscot, SAR imagery of 1992 flood event (light blue), channel layout (dark blue) and gauge station location (red dot).

To develop the discharge recurrence model, a publicly available daily discharge data series at Buscot weir was obtained from the UK National River Flow Archive (see Figure 2). The series spans from 19 years from 1980 to 1998 with some minor gaps that are not expected to affect the extreme statistics analysis to perform.

On the other hand, for the calibration of the inundation model, a satellite observation of the flood extent of 1-in-5 year event occurred in December 1992 was used (see Figure 1). The satellite SAR(synthetic aperture radar) image of the flood was capture 20hs after the flood peak when discharge was at a level of $73m^3/s$ (Aronica et al. (2002)). The resolution of the image is $50m$.

The computational inundation model used is the raster-based Lisflood-fp model (Neal et al. (2012)). Lisflood-fp couples a 2D water flow model for the floodplain and a 1D solver for the channel flow dynamics. Its numerical structure makes it computationally efficient and suitable for the many simulations needed for probabilistic flood risk analysis and model calibration.

A simplified rectangular cross-section is used for the channel with a constant width of 20m for the entire reach and a varying height of around 2m. The observed event is defined by the boundary condition of a fixed input discharge of $v = 73m/s^3$ at the geographic location of the gauging station shown in Figure 1, and by an assumed downstream boundary condition of a fixed water level of approximately 90cm above the channel bed height. The short length of the reach and the broadness of the hydrograph imply that a steady-state hydraulic model is sufficiently accurate for the calibration (Aronica et al. (2002)).

The model's parameters used for calibration are the Manning's roughness parameters for the channel r_{ch} and for the floodplain r_{fp}, both considered spatially uniform in the domain of analysis. That is, $\beta = \{r_{ch}, r_{fp}\}$.

4. RESULTS AND DISCUSSION

4.1. *Models calibration*

A total of 73 extreme events were identified in $18.8yrs$ of data (see Figure 2) using a threshold of $12m^3/s$ and minimum distance between clusters of 7 days. That is approximately $3.9events/year$, and it shows the relative advantage of this type of analysis versus the standard annual maximum approach for which there would only be 18 data points. The posterior distribution of the mean rate λ_o has a mean of $3.8yr^{-1}$ and a standard deviation of $0.44yr^{-1}$. Statistical tests showed that the resulting peaks series is reasonably independent and that the time between events fits reasonably well with an exponential model.

Samples of the GPD parameters were drawn from their posterior (Eq. (7)) by a standard MCMC algorithm of 4 chains of 15,000 samples each. Discarding the first half of sample from each as burn-in stage, convergence of the chains was assessed

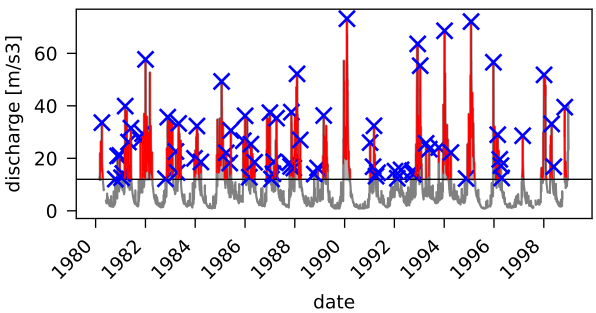

Figure 2: Daily discharge for Buscot and identification of flood events by clustering with a $12\ m/s^3$ *threshold and 7 days of minimum return. Blue cross indicates event's peak discharge.*

by verifying that Gelman-Rubin convergence diagnostic remains below 1.01 (Gelman et al. (2013)). Goodness-of-fit tests showed a good agreement of the exceedances with the model. The shape parameter ξ is centered around -0.05 while the scale parameter σ is centered around 16.5, both with a relatively small skewness

The statistical calibration of the inundation model was done by assuming uniform priors for both parameters in the range $(0.01, 0.15)$ and a threshold of 0.46 to filter out non-behavioral models. This resulted in a bivariate pseudo-posterior distribution for the roughness parameters of the channel and the floodplain as shown in Figure 3. The set of parameters that yield the maximum F-score were $r^*_{ch} = 0.029, r^*_{fp} = 0.045$.

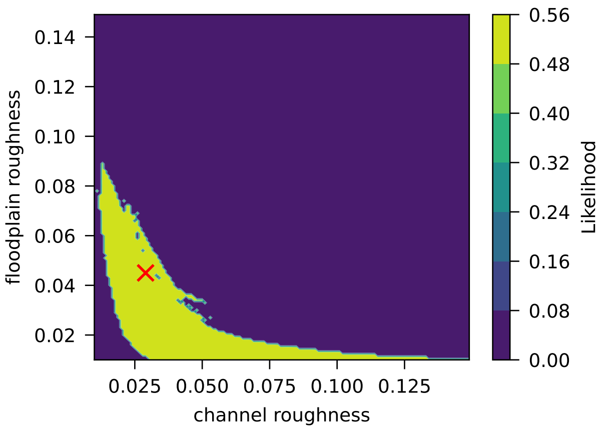

Figure 3: Bivariate posterior distribution for inundation model parameters

4.2. *Flood hazard*

To compute the hazard curve for discharges $\lambda_0 p(\nu|\theta)$, the standard MC algorithm was used and hazard curves were obtained for each sample of θ_i and λ_{0i}. The ensemble of all these possible curves is shown by the 90% uncertainty bounds, and the predictive posterior estimate by the mean (see Figure 4).

A 'deterministic' hazard curve was also computed using the mean posterior λ_0 and the maximum likelihood θ. It can be seen that epistemic uncertainties have the effect of increasing the discharges for a given return period, and that this effect increases with increasing return period. This is intuitive, as larger return periods are more uncertain with limited-length data. Similar results have been obtained by Romanowicz and Kiczko (2016).

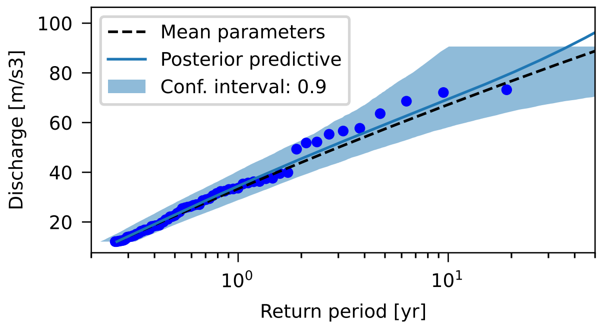

Figure 4: Hazard curves for river discharge

For the flood depth hazard, a simulation time of 5,000yrs was used to obtain a reasonable tradeoff of reliable estimates for hazard up to 1,000yrs return period (Bousquet and Bernardara (2021)), following the approach described in 2.3.

Figure 5 shows the flood depth hazard curve for a point in the floodplain. The posterior predictive curve is compared with the traditional model that uses the deterministic discharge hazard curve (dotted black curve in Figure 4) and a deterministic best-fit inundation simulator using r^*_{ch} and r^*_{fp}. As in the case of the discharge hazard, the predictive posterior appears to give more conservative water depth values than the traditional approach.

This, however, cannot be considered as a general result as it depends on the non-linear nature of the inundation simulator and the calibration processed

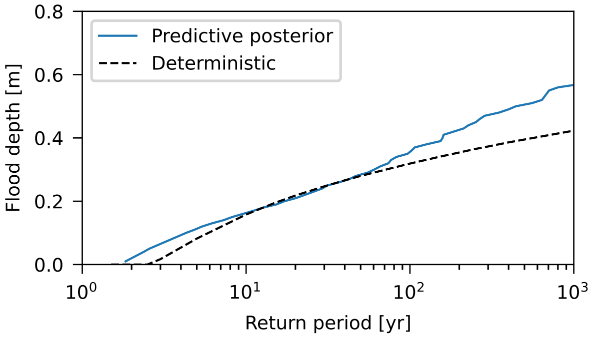

Figure 5: Hazard curves for water depth at location $x = 1.30km, y = 1.05km$

used to obtain the parameters posterior distributions. A flood hazard map for 100yrs was developed by computing the 100yrs flood depth from the posterior predictive curves at each point (see Figure 6). This map is compared in the upper plot of Figure 7 with the traditional hazard map using the deterministic hazard curves. The effect of increasing flood depth for the posterior predictive map can be seen in this figure. This effect, as in the discharge hazard curve, is exacerbated with increasing return periods as can be seen in the lower plot of Figure 7 for the 250yrs maps comparison.

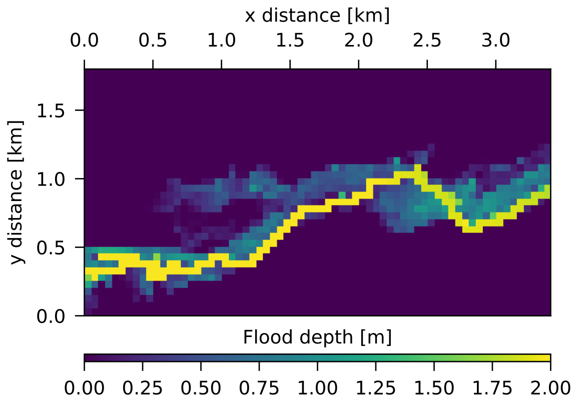

Figure 6: 100yrs flood hazard map using posterior predictive flood depth at each point

5. CONCLUSIONS

The case study showed differences between the predictive posterior estimates and the traditional deterministic ones, that tend to increase with return period. Discharge estimates that include epistemic

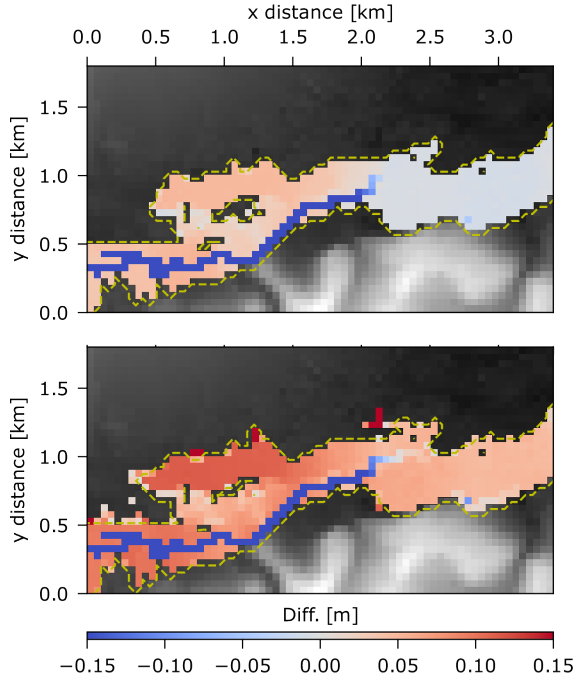

Figure 7: Difference map between posterior predictive estimates and deterministic estimates for 100yrs (upper) and 250yrs (lower)

uncertainty seem to be more conservative, in line with some results in the literature (Romanowicz and Kiczko (2016)). This conclusion, however, cannot be extended immediately to flood depths, since it strongly depends on the inundation simulator and the calibration method used.

While a promising approach, future work needs to further analyze the influence of the inundation simulator and the calibration approach on the posterior predictive estimates of flood hazard and their comparison with the traditional estimates. The larger computational burden should also encourage researchers to find ways of optimizing the simulations, particularly the inundation model component without losing accuracy.

Finally, while the present work used the well-known GLUE method to quantify uncertainty in the inundation model parameters, the distributions obtained are not strictly probabilistic. More formal probabilistic calibration methods are, thus, encorraged to obtain robust probabilistic estimates of hazard and risk as explored in Balbi and Lallemant (2023).

6. REFERENCES

Ahmadisharaf, E., Kalyanapu, A. J., and Bates, P. D. (2018). "A probabilistic framework for floodplain mapping using hydrological modeling and unsteady hydraulic modeling." *Hydrological Sciences Journal*, 63(12), 1759–1775.

Apel, H., Merz, B., and Thieken, A. H. (2008). "Quantification of uncertainties in flood risk assessments." *International Journal of River Basin Management*, 6(2), 149–162.

Aronica, G., Bates, P. D., and Horritt, M. S. (2002). "Assessing the uncertainty in distributed model predictions using observed binary pattern information within GLUE." *Hydrological Processes*, 16(10), 2001–2016.

Aronica, G. T., Candela, A., Fabio, P., and Santoro, M. (2012). "Estimation of flood inundation probabilities using global hazard indexes based on hydrodynamic variables." *Physics and Chemistry of the Earth, Parts A/B/C*, 42–44, 119–129.

Balbi, M. and Lallemant, D. C. B. (2023). "Bayesian calibration of a flood simulator using binary flood extent observations." *Hydrology and Earth System Sciences*, 27(5), 1089–1108 Publisher: Copernicus GmbH.

Beven, K. (2014). *A Framework for Uncertainty Analysis*. IMPERIAL COLLEGE PRESS, 39–59.

Bezak, N., Brilly, M., and Šraj, M. (2014). "Comparison between the peaks-over-threshold method and the annual maximum method for flood frequency analysis." *Hydrological Sciences Journal*, 59(5), 959–977.

N. Bousquet and P. Bernardara, eds. (2021). *Extreme Value Theory with Applications to Natural Hazards: From Statistical Theory to Industrial Practice*. Springer International Publishing, Cham.

Candela, A. and Aronica, G. T. (2017). "Probabilistic Flood Hazard Mapping Using Bivariate Analysis Based on Copulas." *ASCE-ASME Journal of Risk and Uncertainty in Engineering Systems, Part A: Civil Engineering*, 3(1).

Castellanos, M. E. and Cabras, S. (2007). "A default Bayesian procedure for the generalized Pareto distribution." *Journal of Statistical Planning and Inference*, 137(2), 473–483.

Fawcett, L. and Green, A. C. (2018). "Bayesian posterior predictive return levels for environmental extremes." *Stochastic Environmental Research and Risk Assessment*, 32(8), 2233–2252.

Gelman, A., Carlin, J. B., Stern, H. S., Dunson, D. B., Vehtari, A., and Rubin, D. B. (2013). *Bayesian Data Analysis, Third Edition*. CRC Press (November).

Hall, J. and Solomatine, D. (2008). "A framework for uncertainty analysis in flood risk management decisions." *International Journal of River Basin Management*, 6(2), 85–98.

Kennedy, M. C. and O'Hagan, A. (2001). "Bayesian calibration of computer models." *Journal of the Royal Statistical Society: Series B (Statistical Methodology)*, 63(3), 425–464.

Kiczko, A., Romanowicz, R. J., Osuch, M., and Karamuz, E. (2013). "Maximising the usefulness of flood risk assessment for the River Vistula in Warsaw." *Natural Hazards and Earth System Sciences*, 13(12), 3443–3455.

Neal, J., Schumann, G., and Bates, P. (2012). "A subgrid channel model for simulating river hydraulics and floodplain inundation over large and data sparse areas." *Water Resources Research*, 48(11), 1–16.

Nuswantoro, R., Diermanse, F., and Molkenthin, F. (2016). "Probabilistic flood hazard maps for Jakarta derived from a stochastic rain-storm generator." *Journal of Flood Risk Management*, 9(2), 105–124.

Romanowicz, R. J. and Kiczko, A. (2016). "An event simulation approach to the assessment of flood level frequencies: Risk maps for the Warsaw reach of the River Vistula: Event Simulation Approach to Flood Risk Assessment." *Hydrological Processes*, 30(14), 2451–2462.

Stephens, T. A. and Bledsoe, B. P. (2020). "Probabilistic mapping of flood hazards: Depicting uncertainty in streamflow, land use, and geomorphic adjustment." *Anthropocene*, 29, 100231.

Zahmatkesh, Z., Han, S., and Coulibaly, P. (2021). "Understanding Uncertainty in Probabilistic Floodplain Mapping in the Time of Climate Change." *Water*, 13(9), 1248.